



## Experimental designs for optimizing the purification of immunoglobulin G by mixed-mode chromatography



P.L.R. de Sousa<sup>a</sup>, P.A.S. Tavares<sup>a</sup>, E.M.T.S. Teixeira<sup>a</sup>, N.A. Dias<sup>a</sup>, M. de A. Lima<sup>a</sup>, F.M.T. Luna<sup>a</sup>, D.R. Gondim<sup>b</sup>, D.C.S. de Azevedo<sup>a</sup>, I.J. Silva Junior<sup>a,\*</sup>

<sup>a</sup> Universidade Federal do Ceará, Centro de Tecnologia, Departamento de Engenharia Química – Grupo de Pesquisa em Separações por Adsorção – GPSA, Campus do Pici, Bl. 709, CEP: 60455-760 Fortaleza, CE, Brazil

<sup>b</sup> Universidade Estadual Vale do Acaraú, Departamento de Química, Campus Betânia, CEP: 62040-370 Sobral, CE, Brazil

### ARTICLE INFO

#### Keywords:

Protein  
Human serum  
Capto MMC

### ABSTRACT

The main aim of this study was to define the optimal adsorption and elution conditions for the purification of human immunoglobulin G (IgG) by mixed-mode chromatography using the multimodal resin Capto MMC. To this end, Central Composite Experimental Design (ED) was performed for both the adsorption and desorption stages. In the first case, the conditions were systematically studied in batch mode while in the latter case, these were performed in column. For both studies, the experimental design was conducted using high-purity human IgG samples. Buffer pH and concentration as well as the salt concentration were the parameters under study in the ED. Adsorption kinetics and equilibrium experiments were performed under the best conditions defined in the ED (phosphate buffer 60 mmol/L, pH 6.75, no salt). The equilibrium experimental data were fit to the Langmuir equation, with maximum uptake  $q_{max}$  equal to 549.2 mg/g. The  $q_{max}$  value found for IgG in Capto MMC was quite high as compared to other chromatographic techniques that employ single modes of interaction. Regarding elution, the best conditions were obtained with acetate buffer (56.40 mmol/L), pH 5.2 and 0.2 mol/L NaCl. An ultimate recovery of 46.96% for high-purity IgG was achieved. Thus, the effectiveness of Capto MMC for IgG adsorption and recovery could be confirmed. Moreover, electrophoretic runs in the human serum indicated that although co-elution of HSA and IgG proteins occurs, substantial HSA removal and a high IgG recovery were achieved in the elution step.

## 1. Introduction

Immunoglobulin G (IgG) has been widely studied due to its potential use in the treatment of health conditions such as cancer, infectious diseases, autoimmune disorders, among others [1,2]. This can explain the constant search in the pharmaceutical industry for more efficient methodologies to obtain IgG in its pure form. However, the methods currently used comprise two or more steps, which tends to reduce yields and increase process costs. In most cases, the “purification train” includes not only the chromatographic techniques but also some pre- or post-treatment processes [3–5].

Following primary, non-specific pre-treatment protocols, ionic exchange and affinity chromatography are, respectively, the most widely used separation and purification techniques for IgG purification due to the high loading capacities allowed by ion exchange adsorbents and the good interaction of the target biomolecule (IgG) with the active sites of affinity stationary phases. These features render the aforementioned

techniques highly efficient, especially regarding affinity chromatography. Binding of molecules to the stationary phase occurs due to specific interactions between IgG and the ligand attached to the resin, giving rise to high selectivities that are not achieved in ion exchange chromatography. Nevertheless, it is a costly technique and may lead to undesirable phenomena, such as protein aggregation, low stability and eventual denaturation of the target protein or ligand during the elution and regeneration steps of chromatographic runs [4,6]. Table 1 summarizes examples of different materials used in IgG purification assays by means of ion exchange, affinity and mixed-mode chromatography.

Mixed Mode Chromatography (MMC) has recently been recognized as having a great potential for the separation and purification of biomolecules. The technique is based on the capture of the target molecule by multiple interactions, such as ion exchange, hydrophobic interactions, hydrogen bonds and Van der Waals forces, thus increasing the adsorption capacity as compared to single-mode phases. The presence of hydrophobic groups, such as phenyls, grants a salt-tolerance

\* Corresponding author.

E-mail address: [ivanildo@ufc.br](mailto:ivanildo@ufc.br) (I.J.S. Junior).

<https://doi.org/10.1016/j.jchromb.2019.121719>

Received 23 January 2019; Received in revised form 3 July 2019; Accepted 13 July 2019

Available online 16 July 2019

1570-0232/ © 2019 Elsevier B.V. All rights reserved.

**Table 1**  
Materials used for IgG purification.

Interaction type	Material	Reference
Pseudo affinity	Microcomposite composed of bentonite, acrylamide and histidine	[7]
Affinity	HiTrap protein A	[8]
Multimodal charge-induction	W-ABI (tryptophan-5-aminobenzimidazole)	[9]
Ion exchange	Q Sepharose FF/ Poros 50HQ	[10]
Multimodal charge-induction	W-ABI (tryptophan-5-aminobenzimidazole)	[11]
Affinity	Protein G	[12]
Modo misto	Mercapto-Ethyl-Pyridine-Hypercel™	[13]
Affinity biomimetic	FYE-ABI (Phenylalanine-Tyrosine-Glutamate-“5-amino-benzimidazole”)	[14]
Ion exchange – anionic	Diethylaminoethyl (DEAE)	[15]

characteristic to the process [4,15–21]. MMC has been used for the separation of biomolecules of different natures, such as monoclonal and polyclonal antibodies [1,22–24], as well as enzymes [25].

In a recent work, Luo et al. [26] studied the selectivity of four mixed-mode resins (MEP HyperCel, MMI-4FF, ABI-4FF and W-ABI-4FF) with serum fragments of IgG, namely crystallizable fragment (Fc) and antigen-binding fragment (Fab). They concluded that the selectivity of the resins was directly related to the pH of the adsorption step. Regarding IgG, for instance, the best results were obtained at pH close to neutrality (6.0 at 8.9). In addition, by Isothermal Titration Calorimetry (ITC), they could confirm that hydrophobic interactions were predominant.

As mentioned, MMC involves multiple interactions and hence, defining the operating conditions to maximize the retention and elution of the target molecule is of paramount importance. To our best knowledge, there are no studies in the literature that propose to investigate IgG purification using mixed mode resins by Experimental Design (ED) algorithms.

Therefore, the main objective of this study was to apply ED tools to define the best adsorption and elution conditions for the purification of human IgG by Mixed Mode Chromatography. The tested parameters were pH, buffer concentration and salt concentration and experiments were performed both in batch and in fixed bed modes. Subsequently, to demonstrate the performance of the chromatographic runs, experiments with human serum were carried out.

## 2. Experimental section

### 2.1. Materials

Resin Capto MMC was supplied by GE Healthcare (USA). Human immunoglobulin G (IgG) and human serum AB type were obtained from Sigma-Aldrich (USA). Sodium phosphate and sodium chloride were purchased from Vetec (Brazil); sodium acetate and glacial acetic acid were supplied by Dynamics (Brazil) and Synth (Brazil), respectively. The chemicals used in the sodium dodecyl sulphate–polyacrylamide gel electrophoresis (SDS-PAGE) were all supplied by Sigma (USA): acrylamide, bis-acrylamide, SDS and dithiothreitol. All chemicals were of analytical grade and used without further purification. Ultrapure water, required to prepare buffers and other solutions, was obtained using a Milli-Q System (Millipore, USA).

### 2.2. Experimental design

#### 2.2.1. Batch adsorption experiments

A Central Composite Experimental Design (ED) was performed in order to identify the most favorable IgG adsorption conditions. Table 2 presents the range of variables pH, buffer concentration ( $C_{buffer}$ ) and salt concentration ( $C_{salt}$ ) used in the ED. Software *Statistica* (StatSoft, v. 10)

**Table 2**  
Parameters and levels of the central compound planning in the adsorption step.

Parameters	Levels				
	−1.68	−1.00	0.00	+1.00	+1.68
pH	6.00	6.20	6.75	7.20	7.50
$C_{buffer}$ (mmol/L)	20.00	36.00	60.00	84.00	100.00
$C_{salt}$ (mol/L)	0.00	0.20	0.50	0.80	1.00

was used to define the experimental matrix and to analyze the obtained data in order to find the optimum conditions, i.e., those that maximize the response variable, IgG uptake.

The pH values chosen for the ED were based on the pI of IgG which, according to the literature, ranges between 6.3 and 9.0 [27]. Sodium phosphate buffer was then chosen because of its buffering range (pH 5.8–8.0).

The experiments were conducted in vials placed in an orbital stirring system (TECNAL, model TE-165, Brazil) at 30 rpm and room temperature for 1.5 h. In each vial, 3 mL IgG solution in 1.0 mg/mL sodium phosphate buffer were mixed with 10 mg resin. Thereafter, a 2-mL sample was collected and centrifuged at 9998 xg for 10 min. Then, the absorbance of the supernatant at 280 nm was measured in a UV-VIS spectrophotometer. The adsorbed concentration of IgG (response variable) was calculated according to Eq. (1):

$$q^* = \frac{V_{sol}(C_0 - C_{eq})}{m_{ads}} \quad (1)$$

where  $q^*$  is the adsorbed concentration of protein (mg/g);  $C_{eq}$  is the protein concentration in the liquid phase (mg/mL) at equilibrium with the solid phase;  $C_0$  is the initial protein concentration in the liquid phase (mg/mL);  $m_{ads}$  is the mass of adsorbent (g) and  $V_{sol}$  is the volume of protein solution (mL) added to the vial.

Following the identification of the best adsorption conditions, kinetic experiments were performed under those conditions to verify the time required to reach equilibrium for human IgG adsorption onto Capto MMC. The experiments were performed with three initial protein concentrations (1.0, 2.0 and 3.0 mg/mL) and uptake times ranged from 0 to 240 min.

The parallel diffusion model (Eqs. (2)–(6)) was used to estimate the contribution of mass transfer parameters in the kinetics of human IgG adsorption onto Capto MMC resin. It was assumed that diffusion in the pore and in the surface occur simultaneously.

Mass balance in the resin particle:

$$\varepsilon_p \left( \frac{\partial C_i}{\partial t} \right) + D_{ap} \frac{\partial q_i}{\partial t} = \varepsilon_p D_p \left( \frac{\partial^2 c_i}{\partial r^2} + \frac{2}{r} \frac{\partial c_i}{\partial r} \right) + D_s D_{ap} \left( \frac{\partial^2 q_i}{\partial r^2} + \frac{2}{r} \frac{\partial q_i}{\partial r} \right) \quad (2)$$

where  $D_p$  and  $D_s$  are, respectively, the diffusion coefficients in the pore and on the surface.

Boundary conditions:

$$r = 0; \frac{\partial c_i}{\partial r} = 0 \quad (3)$$

$$r = R; \varepsilon_p D_p \frac{\partial c_i}{\partial r} + D_{ap} D_s \frac{\partial q_i}{\partial r} = kf(c_b - c_i) \quad (4)$$

Mass balance in liquid phase:

$$\frac{\partial c_b}{\partial t} = - \left( \frac{3vk_f}{RV} \right) (c_b - c_i) |_{r=R} \quad (5)$$

Initial conditions:

$$t = 0; c_b = c_0 \quad (6)$$

where  $C_b$  is the total concentration of proteins in the liquid phase,  $k_f$  is the mass transfer coefficient through the liquid film,  $R$  is the particle radius,  $v$  is the volume of the adsorbent and  $V$  is the volume of liquid.

The  $k_f$  and  $D_{AB}$  were estimated according to Geankoplis [28] (Eqs. (7) and (8)) and used as input values of the model:

$$k_f = \frac{2D_{AB}}{d} + 0.31 \left( \frac{\mu}{\rho D_{AB}} \right)^{-\frac{2}{3}} \left( \frac{\Delta\rho\mu g}{\rho^2} \right)^{\frac{1}{3}} \quad (7)$$

where  $D_{AB}$  is the molecular diffusivity,  $d$  is the particle diameter,  $\mu$  is the viscosity of the solution,  $\rho$  is the particle density,  $\Delta\rho$  is the difference between the particle density and the solution and  $g$  is the acceleration due to gravity.

$$D_{AB} = 9.4 \cdot 10^{-15} \frac{T}{\mu (M_A)^{\frac{1}{3}}} \quad (8)$$

where  $M_A$  is the molecular weight of the protein and  $T$  is the absolute temperature.

The model was solved numerically using the gPROMS commercial solver (Version 3.2). The radial domain was discretized using a third-order orthogonal collocation method in finite elements. The estimation of the mass transfer parameters ( $D_p$  and  $D_s$ ) in batch mode was performed by an optimization subroutine using the heterocedastic method [29].

To measure the adsorption equilibrium isotherms under the optimal pH,  $C_{buffer}$  and  $C_{salt}$  conditions identified, the default time to reach equilibrium was taken to be 3 h. The initial protein concentration ranged between 0.5 and 6.0 mg/mL. The Langmuir equation was used to fit the experimental data (Origin® software, Microcal, USA), according to Eq. (9):

$$q = \frac{q_{max} k C_{eq}}{1 + k C_{eq}} \quad (9)$$

where  $q_{max}$  is the theoretical maximum adsorbed concentration (mg/g);  $k$  is the adsorbent-adsorbate interaction constant (mL/mg) and  $C_{eq}$  is the equilibrium concentration (mg/mL) in the liquid phase.

### 2.2.2. In-column desorption

A new central composite experimental design was performed in order to obtain the best conditions for the elution (desorption) step. Table 3 shows the levels attributed to each variable under study. According to the literature [26], pH, acetate buffer concentration ( $C_{buffer}$ ) and salt concentration ( $C_{salt}$ ) should be used as independent variables. For the elution assays, acetate buffer was used because the pH range differed from that in the adsorption step.

The tests were performed in a chromatographic system consisting of a peristaltic pump (WATSON MARLOW, Brazil), a glass column C10/10 from GE (10 cm × 10 mm) and a fraction collector (BUCHI C-660, Switzerland). 250 mg dry Capto MMC were packed into the column so as to obtain a bed length of 1.6 cm. Subsequently, 10 mL of a 1 mg/mL IgG solution was prepared under the optimal pH and buffer conditions previously identified for adsorption. This solution was pumped into the column under a flow rate of 0.8 mL/min. After 10 min, the column was submitted to a washing step by changing the feed to pure buffer under the same conditions as those in the adsorption step. For the elution, the conditions defined by the ED (Table 3) were used. Between two successive chromatographic runs, a NaOH solution (1 mol/L) would flow through the column for regeneration purposes. In total, 17

**Table 3**

Parameters and levels of the central compound experimental design in the elution step.

Parameters	Levels				
	-1.68	-1.00	-1.68	+1.00	-1.68
pH	3.60	4.10	4.60	5.20	5.60
$C_{buffer}$ (mmol/L)	20.00	56.40	110.00	163.60	200.00
$C_{salt}$ (mol/L)	0.00	0.200	0.50	0.80	1.00

chromatograph experiments were performed. Note that the adsorption, washing and regeneration steps were identical, following previously optimized conditions; only the elution step was carried out according to the conditions described in Table 3. The IgG recovery was then calculated according to Eq. (10):

$$IgG \text{ Recovery (\%)} = \frac{\text{Eluted IgG (mg)}}{\text{Injected IgG (mg)}} \times 100 \quad (10)$$

### 2.3. Purification of IgG from human serum

Once the optimal conditions regarding the adsorption and elution steps were identified, chromatographic experiments were performed for IgG purification from human serum using a Contichrom system (Knauer, Germany). 250 mg Capto MMC were packed into the column and 10 mL of 5 mg/mL human serum diluted in 60 mmol/L phosphate buffer at pH 6.75 were injected into the column. Then, the column was rinsed with 10 mL of 60 mmol/L phosphate buffer at pH 6.75. Finally, elution was performed with 0.2 mol/L NaCl in 56.4 mmol/L sodium acetate buffer at pH 5.2. During all experiments, samples were collected at the outlet of the columns for electrophoresis assays and quantification by the Bradford method.

### 2.4. Analytical methods

#### 2.4.1. Total protein quantification

The total protein content was analyzed according to the procedure described by Bradford [30] using Bovine Serum Albumin (BSA) as the reference protein and Coomassie blue for color development. The intensity of the color was measured at 595 nm using a UV-Visible spectrophotometer (Thermo Scientific, USA).

#### 2.4.2. Electrophoresis assays

SDS-PAGES of protein samples were performed under denaturing and reducing conditions [31] using a Mini-Protean III System (Bio-Rad, USA). The runs were carried out at 150 V in 7.5% separation gels with a 4% stacking gel. Protein bands were revealed with Coomassie Blue.

## 3. Results and discussion

### 3.1. Batch adsorption experiments

Seventeen batch adsorption experiments were performed to define the pH, buffer concentration and salt concentration that would maximize IgG uptake. Table 4 shows the values of adsorbed protein

**Table 4**

Batch adsorption experiments with Capto MMC for IgG adsorption using sodium phosphate buffer at different condition.

Test	pH	$C_{buffer}$ (mmol/L)	$C_{salt}$ (mol/L)	q (mg/g)
1	6.20	36.00	0.20	116.91
2	6.20	36.00	84.00	58.67
3	6.20	84.00	0.20	116.06
4	6.20	84.00	84.00	102.06
5	7.20	36.00	0.20	67.20
6	7.20	36.00	84.00	96.14
7	7.20	84.00	0.20	80.97
8	7.20	84.00	84.00	82.49
9	6.00	60.00	0.50	122.27
10	7.50	60.00	0.50	73.53
11	6.75	20.00	0.50	77.13
12	6.75	100.00	0.50	83.89
13	6.75	60.00	0.00	223.28
14	6.75	60.00	1.00	103.20
15	6.75	60.00	0.50	80.05
16	6.75	60.00	0.50	73.11
17	6.75	60.00	0.50	84.68

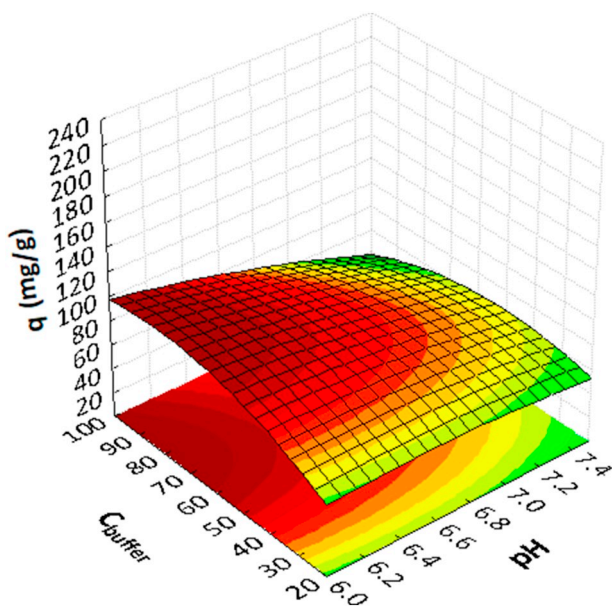


Fig. 1. Response Surface for adsorption step with variations of pH and buffer concentration and salt concentration in central point (0.5 mol/L).

obtained in each run of the ED for the adsorption step. The IgG solution was diluted in sodium phosphate in all the experiments.

The experimental condition with the highest concentration of adsorbed IgG (223.28 mg/g of IgG adsorbed) was achieved under the following conditions: pH 6.75,  $C_{buffer}$  60.0 mmol/L and  $C_{salt}$  0.0 mol/L. Figs. 1 to 4 illustrate the Response Surfaces and the Pareto Diagram obtained from Statistica by handling of the results shown in Table 4.

The results were consistent with those reported in the literature, since most biomolecules tend to show favorable binding conditions close to their respective pI. The pI of IgG falls within the range of 6.3 to 9.0 [28]. Joucla et al. [32] carried out IgG adsorption experiments in phosphate buffer (0.1 mmol/L) at pH 6.8, conditions similar to those found in the present study, except for the buffer concentration.

Gospodarek et al. [33] investigated the interactions between Capto MMC and bovine serum albumin (BSA) by hydrogen exchange mass spectrometry (HXMS). They tried to relate the BSA pI with the solution

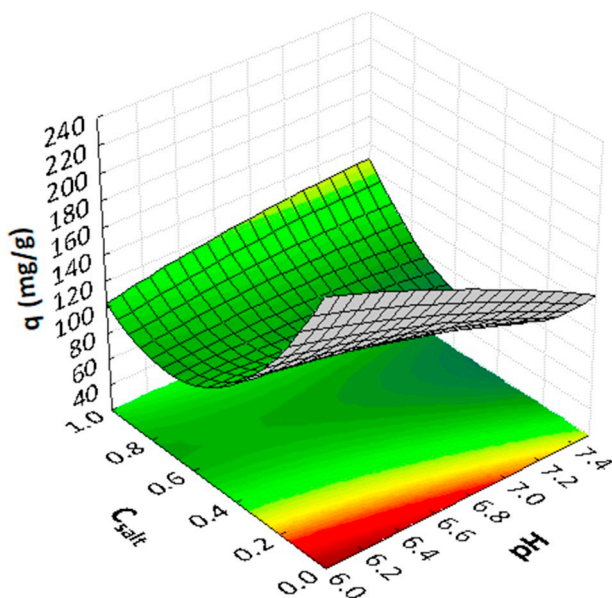


Fig. 2. Response Surface for adsorption step with variations pH and salt concentration and buffer concentration in central point (60.00 mmol/L).

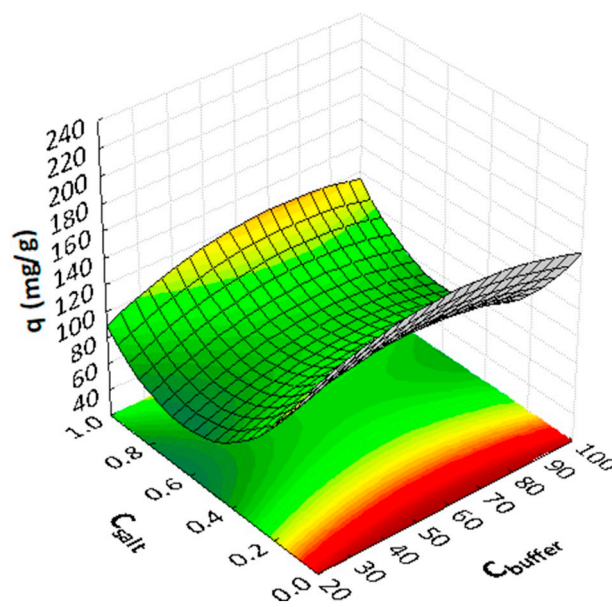


Fig. 3. Response Surface for adsorption step with variations buffer and salt concentrations and pH in central point (6.75).

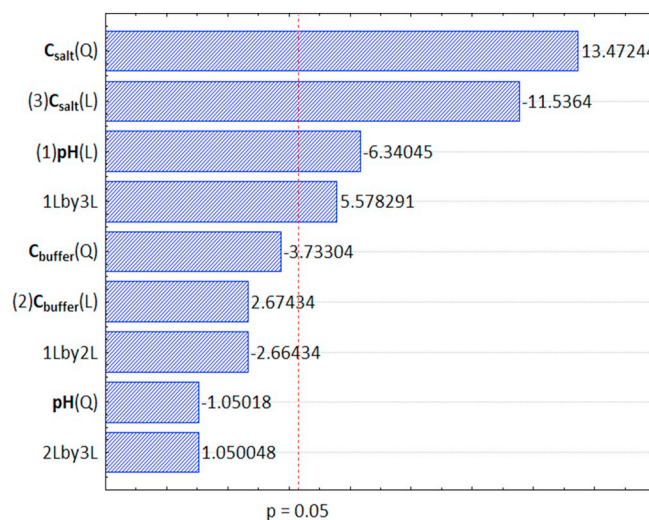


Fig. 4. Pareto diagram, at 95% of significance, for central compound experimental design adsorption step.

pH and ionic strength (50 mmol/L ammonium sulfate). By increasing the ionic strength (0.5 to 1.5 mol/L) and adjusting the pH to the pI of BSA, the electrostatic interactions were decreased and hydrophobic interactions were favored.

A relevant observation was made regarding  $C_{salt}$ , since the highest protein uptake was obtained in salt-free conditions. This fact suggests that, although Capto MMC comprises different modes of interaction, ion exchange appear to be the governing chromatographic mechanism. Also, according to the Pareto Diagram,  $C_{salt}$  is the most significant variable to influence the adsorbed concentration  $q$ , followed by pH. Inside the range of the experimental conditions considered, the best protein uptakes were obtained at the lowest values of  $C_{salt}$  and pH. As for  $C_{buffer}$ , no consistent trends could be observed.

The kinetic experiments were carried out under the conditions of maximum protein uptake found by the ED (pH 6.75,  $C_{buffer}$  60.00 mmol/L,  $C_{salt}$  0.00 mol/L). The input parameters used for the parallel diffusion model are shown in Table 5. The coefficients  $k_f$  and  $D_{AB}$  were obtained using Eqs. (7) and (8), respectively. The particle porosity was found by Lima et al. [34].

**Table 5**  
Parameters inserted in the parallel diffusion model.

Parâmetros	Capto MMC
Porosity of the particle, $\epsilon_p$	0.55 <sup>a</sup>
Density of the particle, $D_a$ (g·cm <sup>-3</sup> )	1.5
Particle diameter, $d$ (cm)	$3.75 \cdot 10^{-3}$
Coefficient of molecular diffusion, $D_{AB}$ (cm <sup>2</sup> ·min <sup>-1</sup> )	$3.39 \cdot 10^{-5}$
Coefficient of mass transfer in the film, $k_f$ (cm·min <sup>-1</sup> )	0.188

<sup>a</sup> Source: [34].

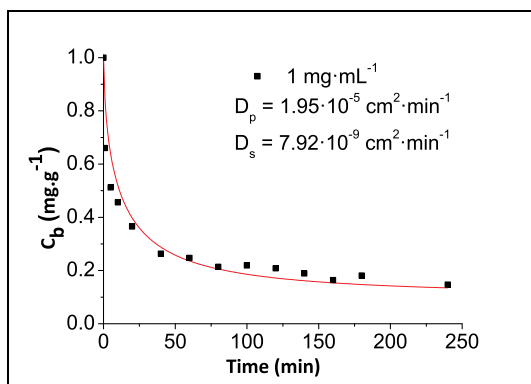


**Fig. 5.** Kinetic Profile Modeling to IgG ( $C_i = 1 \text{ mg}\cdot\text{mL}^{-1}$ ) using Capto MMC resin.

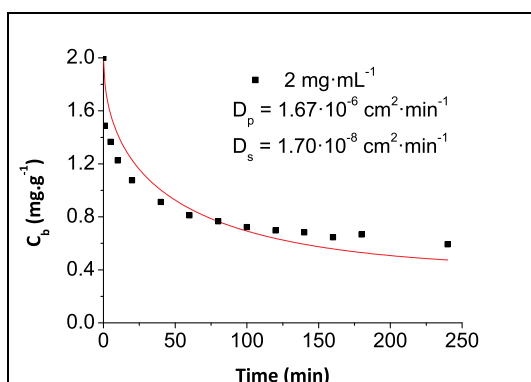


**Fig. 6.** Kinetic Profile Modeling to IgG ( $C_i = 2 \text{ mg}\cdot\text{mL}^{-1}$ ) using Capto MMC resin.

In Figs. 5 to 7, the experimental and the simulated kinetic profiles are depicted. The parallel diffusion model was employed to simulate the adsorption kinetics data at different concentrations (1, 2 e 3 mg·mL<sup>-1</sup> of IgG). The estimated values of  $D_p$  and  $D_s$  indicated the predominance of pore diffusivity, since  $D_p$  values ranged from  $1.95 \cdot 10^{-5}$  to  $1.67 \cdot 10^{-6} \text{ cm}^2 \cdot \text{min}^{-1}$ . The values of  $D_s$  varied from  $7.92 \cdot 10^{-9}$  to  $1.7 \cdot 10^{-8} \text{ cm}^2 \cdot \text{min}^{-1}$ . In addition, it has been noticed that the diffusivities tend to decrease with increasing IgG concentration. Zhu and Carta [35] noticed a similar behavior when adsorption kinetics for lysozyme and mAb were investigated at different salt concentrations with the mixed mode resins Nuvia cPrime and Capto MMC. They also noticed that the apparent diffusivity ( $D_e$ ) values found for these proteins are independent of the salt concentration for both resins. For lysozyme, operating at pH 5.0 and in the absence of NaCl, the authors obtained  $D_e$  values of  $0.16 \cdot 10^{-5} \text{ cm}^2 \cdot \text{min}^{-1}$  and  $0.96 \cdot 10^{-5} \text{ cm}^2 \cdot \text{min}^{-1}$  for the mixed mode resins Nuvia cPrime and Capto MMC, respectively. On the other hand, for mAb, the diffusivities were 3-fold lower when compared to those presented by lysozyme ( $0.4 \cdot 10^{-5} \text{ cm}^2 \cdot \text{min}^{-1}$  and  $0.78 \cdot 10^{-6} \text{ cm}^2 \cdot \text{min}^{-1}$  for Nuvia cPrime and Capto MMC, respectively). The lower mass transfer rates obtained with Capto MMC were

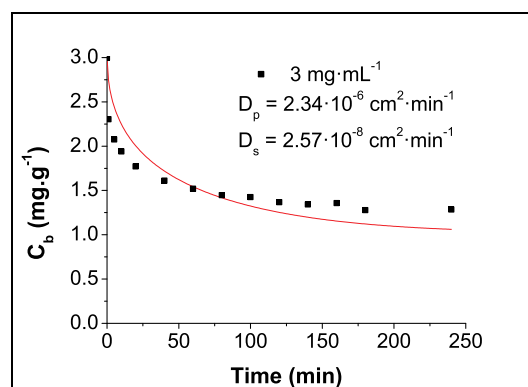


**Fig. 7.** Kinetic Profile Modeling to IgG ( $C_i = 3 \text{ mg}\cdot\text{mL}^{-1}$ ) using Capto MMC resin.

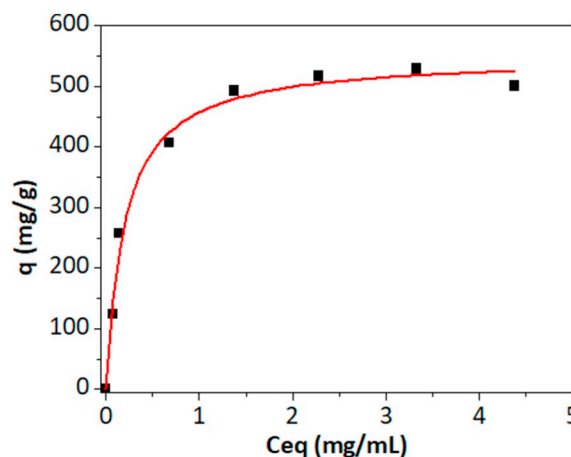


**Fig. 8.** Adsorption equilibrium isotherm at room temperature for IgG in capto MMC under the best conditions defined by experimental design (pH 6.75,  $C_{\text{buffer}} 60.00 \text{ mmol/L}$ ,  $C_{\text{salt}} 0.00 \text{ mol/L}$ ). The continuous curve stands for the regression of experimental data with the Langmuir model.

associated to its smaller pore size when compared to that of Nuvia cPrime. In the addition, the presence of diffusional impedance was observed in Capto MMC, which was related to the size of the mAb molecule: the higher the mAb concentration the lower the diffusivity in Capto MMC, and vice versa.

The curves show that the highest mass transfer rates occurred in the initial minutes; the concentration of IgG in solution was reduced to less than 50% in the first 5 min for most experiments. The transfer rates would then slow down, and equilibrium was reached after 180 min, when the IgG concentrations in the liquid phase had been reduced by about 90% (1 mg/mL), 70% (2 mg/mL) and 50% (3 mg/mL). It can also be stated that the equilibrium time was not affected by initial concentration, since the all the curves presented very similar behavior patterns.

Fig. 8 shows the equilibrium adsorption isotherm at room temperature and the curve plotted represents the data fit to the Langmuir model. It can be observed that after the plateau was reached, the adsorption capacity was identified to be  $549.2 \text{ mg}\cdot\text{g}^{-1}$ ,  $k$ -value  $4.97 \text{ mL}\cdot\text{mg}^{-1}$  and  $R^2 0.99$ . The IgG adsorbed concentration was relatively high, since this represented nearly 50% of the resin mass, what showed that IgG might have had its interactions with Capto MMC enhanced with the use of a suitable buffer, pH and a salt-free liquid-phase. When evaluating the adsorption capacity, the Capto MMC and Nuvia cPrime for lysozyme at pH 3.0, 5.0 and 7.0 and adding NaCl at concentrations of 0.0, 200 and 400 mmol·L<sup>-1</sup>, Zhu and Carta [35] verified that the pH as well as the salt concentration interfere with the

adsorption isotherm. This behavior was explained by the multimodal nature of the resins and their salt-tolerance effect. The maximum capacity reached was  $130 \text{ mg}\cdot\text{mL}^{-1}$  for Capto MMC, when at pH 7.0 and with no added NaCl. Regarding Nuvia cPrime, a  $q_m$  of  $110 \text{ mg}\cdot\text{mL}^{-1}$  was obtained at pHs 5.0 and 7.0 and in the absence of NaCl. For both resins, the  $q_m$ -values are lower than that obtained for IgG on Capto MMC. However, when compared to other types of materials, maximum capacities much higher than those found in this work can be observed. A class of synthesized and functionalized materials, known as SBA-15, have been evaluated for protein capture and the adsorption capacities reported are higher than those for Capto MMC. This is apparently due to synthesis conditions, which grant the material a very large and well-defined pore structure. For example, Bazzaz et al. [36] obtained a  $q_{\text{max}}$  of  $1000 \text{ mg/g}$  for BSA in the hexagonal mesoporous silicate material loaded with APTES and tannin. Acet et al. [37] obtained a  $q_{\text{max}}$  of  $1275.2 \text{ mg/g}$  for lysozyme in  $\text{Cu}^{+2}$ -SBA-15 nanoparticles.

The initial slope of the adsorption isotherm also suggests that human IgG shows a strong interaction with Capto MMC. This fact may be related to the multiplicity of possible interactions between the adsorbent and the biomolecule (ion exchange, hydrophobic interactions, Van der Waals forces and hydrogen bonds), although ion exchange seems to be the predominant modality. Li and Sun [38] developed a multimodal poly (4-vinylpyridine) polymer binder for protein application. A decrease in adsorption capacity was observed when the  $C_{\text{buffer}}$  was increased, indicating that electrostatic interactions between the adsorbent and proteins are predominant. In Capto MMC, hydrophobic interactions are likely to play a secondary role. However, their presence contributed to the salt tolerance characteristic of the adsorbent. Joucla et al. [32], studying capture of mAb in Capto MMC, found that, at pH 5.0, the increase in conductivity was not significant for antibody capture due to the ligand being salt tolerant. This means that an increased conductivity reduces ion exchange interactions at the same time that it favors hydrophobic interactions. However, higher mAb retention could also be achieved for lower conductivities, which is associated with the predominance of ion exchange interactions in the ligand Capto MMC.

### 3.2. In-column desorption

The elution experiments were carried out in fixed bed with sodium chloride added to acetate buffer at different molar concentrations in the elution step (as described in Section 2.2.2), in order to find the best condition for maximizing IgG recovery. Figs. 9 to 12 show the Response Surfaces and the Pareto Diagram for the elution step of human IgG. The recovery was calculated by a mass balance in the liquid phase.

The response surfaces indicate that the best elution conditions are found at the highest pH and  $C_{\text{salt}}$  ranges. For  $C_{\text{buffer}}$ , as previously observed in the ED performed for adsorption, no outstanding trends were observed. According to the statistical treatment of the data, all variables studied were significant, with  $C_{\text{salt}}$  showing the strongest influence on IgG recovery, followed by the interaction between pH and  $C_{\text{buffer}}$ . This behavior suggests that under these conditions, ion exchange interactions predominantly govern the IgG adsorption and desorption on Capto MMC.

The IgG recoveries obtained in the fixed bed experiments are shown in Table 6. Run 5 (pH 5.2;  $C_{\text{buffer}}$  56.4 mmol/L;  $C_{\text{salt}}$  0.2 mol/L) yielded the highest recovery percentage of IgG (47%). Yang et al. [39], studying IgG adsorption on the resin Nuvia cPrime, were able to obtain recoveries of above 80%. In their work, however, much more drastic conditions were used, when compared to those in our study: 0.8 mol/L  $(\text{NH}_4)_2\text{SO}_4$  buffer at pH 8.0 and 1.0 mol/L NaCl for the elution stage. This set of conditions could impart higher processing costs due to the need for posterior desalting operations.

Statistical handling of the data showed that among all the variables studied in the adsorption and elution stages of IgG, salt concentration was the most significant parameter. The best adsorption condition

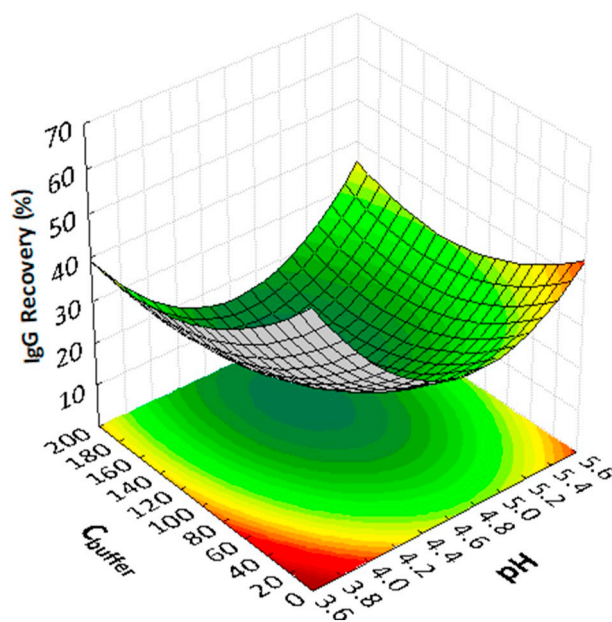


Fig. 9. Response Surface for elution step with variations pH and buffer concentration and salt concentration in central point (0.5 mol/L).

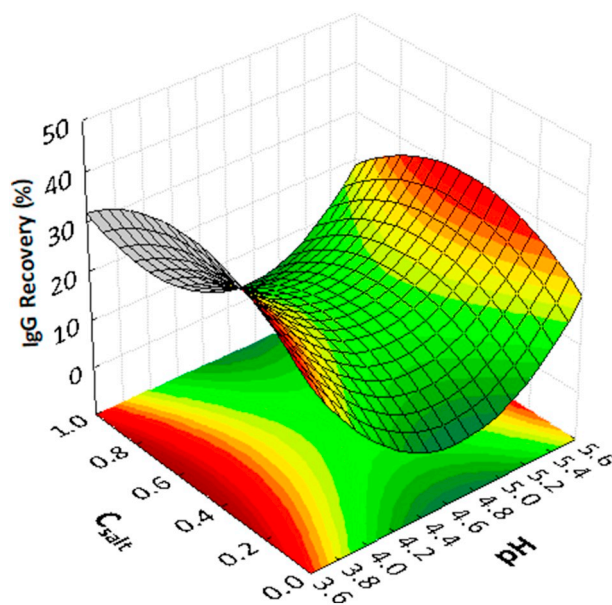


Fig. 10. Response Surface for elution step with variations pH and salt concentration and buffer concentration in central point (110 mmol/L).

occurred in the absence of salt and, for elution, this happened in the highest salt concentration tested. This fact seems to confirm the hypothesis that ion exchange is in fact the predominant interaction taking place between IgG and Capto MMC. Luo et al. [11] obtained similar results by using the adsorbent MMI-4FF (2-mercapto-1-methyl-imidazole) in the separation of IgG from Fc-fragments when operating under pH 6.0 for adsorption and pH 3.0 (48.0%) and 4.0 (41.9%) for desorption. Even better results (86.5%) were observed when the resin Trtptophan-5-aminobenzimidazole (W-ABI-4FF) was employed at pH 8.0 for loading and 3.6 for elution. These materials differ in the number of aromatic rings of the ligands and consequently, present different hydrophobicities. Also, elution of IgG is likely to be strongly influenced by salt concentration gradients. In fact, Maria et al. [23] reported the successful elution of IgG when using pH and a buffer conductivity gradient for Capto MMC. As shown in the Pareto Chart

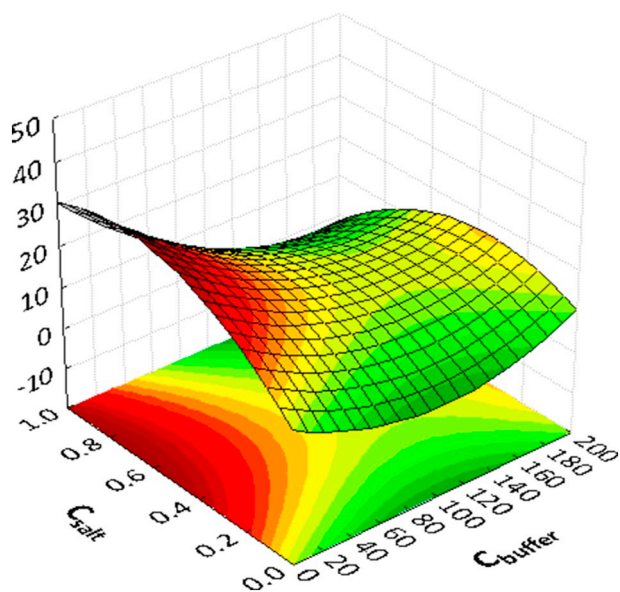


Fig. 11. Response Surface for elution step with variations Buffer and salt concentrations and pH in central point (4.6).

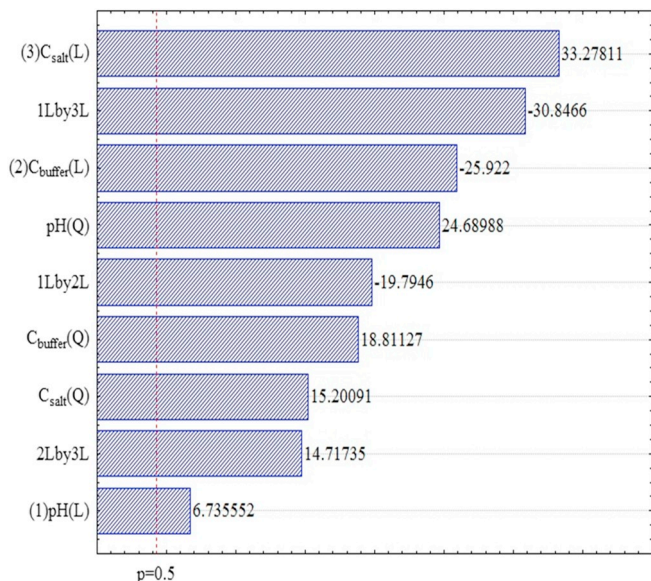


Fig. 12. Pareto diagram, at a 95% of significance, for central compound experimental design elution step.

(Fig. 12), salt concentration was the most significant variable, followed by the interaction thereof with the pH.

By solely considering the recovery percentage, the overall yield is in fact lower than those found in a few other studies available in the literature. Tong et al. [40] report recoveries of around 85% with a hydrophobic interaction resin and Wang et al. [41], of 95% with a mixed mode adsorbent, both working with IgG from BSA. Specifically targeting HSA, Bresolin et al. [27] obtained an IgG recovery of 75% with a mixed-mode agarose-based ligand. Nevertheless, apart from reiterating that using Capto MMC for purifying human IgG has never been approached and hence, the present study serving as a valid addition to the already-existing knowledge, future work can focus on refining this process for improving the results obtained, either by fine-tuning other process parameters or by adding downstream unit operations to the protocol, such as membrane technologies [42].

Table 6  
Recovery percentages in the elution step of IgG.

Experiment	pH	C <sub>buffer</sub> (mmol/L)	C <sub>salt</sub> (mol/L)	IgG recovery (%)
1	4.10	56.40	0.20	10.20
2	4.10	56.40	0.80	44.96
3	4.10	163.60	0.20	7.51
4	4.10	163.60	0.80	40.25
5	5.20	56.40	0.20	46.96
6	5.20	56.40	0.80	30.97
7	5.20	163.60	0.20	5.34
8	5.20	163.60	0.80	22.85
9	3.60	110.00	0.50	8.79
10	5.60	110.00	0.50	18.08
11	4.60	20.00	0.50	14.24
12	4.60	200.00	0.50	5.14
13	4.60	110.00	0.00	0.26
14	4.60	110.00	1.00	14.52
15	4.60	110.00	0.50	8.28
16	4.60	110.00	0.50	6.80
17	4.60	110.00	0.50	7.81

### 3.3. Purification of IgG from human serum

Chromatographic experiments with human serum samples diluted in phosphate buffer (60 mmol/L) and at pH 6.75 were performed. The adsorption step consisted in injecting 1 mL of human serum (at 5.0 mg/mL in buffer); the washing step was performed with pure phosphate buffer and the elution was carried out with NaCl (at 0.2 mol/L) added of acetate buffer (56.4 mmol/L), at pH 5.2.

Fig. 13 shows the UV-absorbance (280 nm) at the exit of the column for the chromatographic run in the FPLC - Contichrom using the resin Capto MMC under the conditions previously described.

The peak observed in the regeneration (R) step stands out in the profile and is much higher than that observed in the elution (E) step. Apparently, most of the adsorbed proteins (IgG and HSA) are recovered at point R rather than in E, which is consistent with the relatively low recoveries (below 50%) observed in the fixed bed experiments with pure IgG.

Yang et al. [20] investigated the co-adsorption of IgG and Bovine Serum Albumin (BSA) using the multimodal resin Nuvia cPrime as the adsorbent. Their results also indicated high adsorption for both proteins in pHs ranging from 6.0 to 8.0, which is very close to the pI of the IgG. IgG showed higher adsorption for all the tests. Tong et al. [9] also performed experiments using a multimodal W-ABI resin modified by induction charges to purify IgG from a mixture solution with BSA. Separation was achieved with elution with acetate buffer in the pH range 4.5–5.0, which yielded IgG with a purity degree of 95.2% and of 98.4%, if adding 0.1 M NaCl to the loading buffer. By utilizing a similar starting material, it was possible to recover 88.1–89.9% of IgG from the resin MEP HyperCel.

One factor that might have contributed for the recovery value of IgG obtained in this work (~47%) is the structural form and the binding energy of the protein with Capto MMC. The IgG molecule is “Y”-shaped, what makes it difficult to access the adsorbent pores. This is reinforced by observing the results of the kinetic modeling, which showed that although pore diffusion is indeed predominant, surface diffusion also occurs. HSA, on the other hand, is a much smaller protein, presenting small molecular weight and globular structure, thus facilitating its access to the pores. Also, it could be verified that HSA possesses much higher adsorption energy in Capto MMC when compared to IgG (data not shown), deeming its separation more difficult. Although a large amount of proteins still seems to remain bound to the resin during the elution step, it is important to assess the relative concentration of IgG and HSA (i.e., resin selectivity) present in the elution fraction collected.

The electrophoresis assay of the various fractions collected is depicted in Fig. 14. It is noticeable that the elution conditions applied were able to deliver fractions that are free from some of the proteins

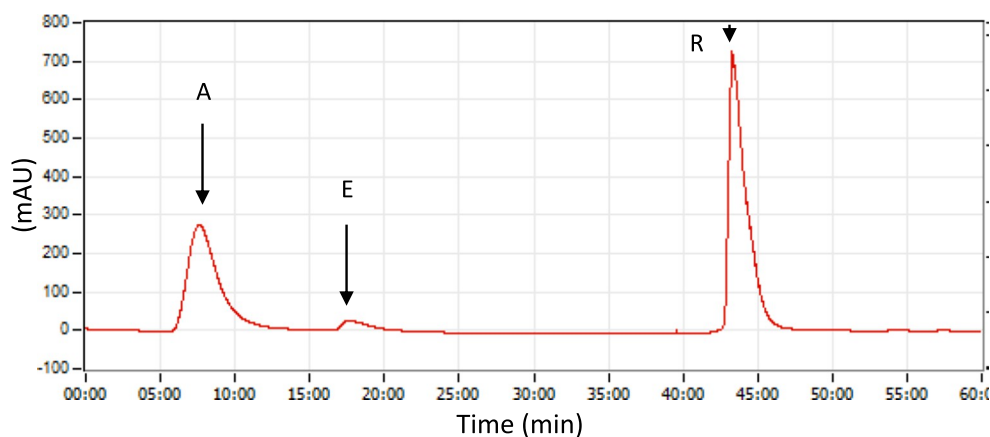


Fig. 13. UV-absorbance ( $\lambda = 280$  nm) profile at the column exit for a chromatographic run of human serum proteins. Conditions: Adsorption (Phosphate buffer 60 mmol/L pH 6.75), Elution (Acetate sodium 56.4 mmol/L pH 5.2 NaCl 0.2 mol/L), Regeneration (NaOH 1.0 mol/L). Samples collected at different moments: (A) Adsorption; (E) elution; (R) regeneration.

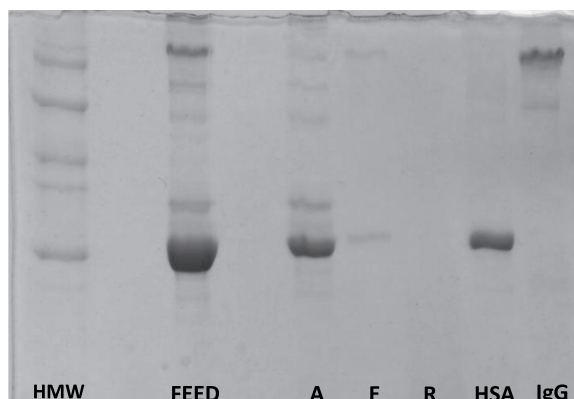


Fig. 14. Electrophoresis related to chromatographic run with human serum in Capto MMC in Contichrom. HMW: High molecular weight standard; FEED: Sample of human serum used in the tests; A: Adsorption; E: Elution; R: Regeneration; HSA: Human Serum Albumin; IgG: immunoglobulin G.

present in human serum, particularly those of intermediate molecular weight. However, IgG could not be completely purified, since human serum albumin (HSA) can still be found in the eluted fraction. In fact, Yan et al. [21] also concluded that, for the resin Nuvia cPrime, the most favorable adsorption and elution conditions were very similar for both IgG and HSA, which can lead to constant 'contamination' during all stages. No proteins were identified in the regeneration (R) stage due to the high concentration of NaOH used.

The results for adsorption and desorption reported in this work for Capto MMC can provide a useful guide for an unrefined separation of IgG from most of the human serum proteins. For finer applications, where complete IgG purification is required, other chromatographic operations can be useful additions, such as affinity chromatography or the testing of other buffer conditions of ionic strength or pH. In this case, further data on HSA adsorption equilibrium and kinetics in the target stationary phase is required. In this work, however, it was already possible to obtain a fraction much purer than the raw sample used for loading the system. As such, the resin can be undoubtedly used to greatly reduce the number of interferences and, additionally, other specific chromatographic processes can be performed aiming at completely purifying IgG. Thus being, the purity degree of the protein could be potentially increased along with process yields due to the considerable decrease in the number of contaminant proteins.

#### 4. Conclusion

The experimental designs in tandem with the statistical tools employed in this work were useful for defining the operating conditions

(pH, buffer and salt concentration) that enhanced and optimized the adsorption and recovery (upon elution) of human IgG using the multimodal chromatographic resin Capto MMC. These conditions allowed a recovery of about 50% (w/w) of relatively-pure IgG.

When an actual sample of human serum was tested under the optimal adsorption/desorption conditions previously identified, the IgG could be successfully separated from most serum proteins, except from HSA. In case complete purity is required, there is a need for further investigation onto the co-elution of these proteins.

Finally, this study was a good addition to the knowledge by revealing the prevailing modalities of interactions between IgG and Capto MMC, which were found to be of ion-exchange nature, despite the concurrence of other types of interaction inherent in the multimodal resin.

#### Transparency document

The [Transparency document](#) associated with this article can be found, in online version.

#### Acknowledgments

The authors gratefully acknowledge the grants received from *Fundação Cearense de Apoio ao Desenvolvimento Científico e Tecnológico* (FUNCAP: PEP-0094-00001.01.125-15) and the financial support by *Conselho Nacional de Pesquisa* (CNPq: 479942/2013-7 and 455215/2014-6).

#### References

- [1] Dong, Y.; Pang, B.; Yu, F.; Li, L.; Liu, W.; Xiu, Z. *J. Chromatogr.* 1012–1013 (2016) 137–143.
- [2] E. Melnik, R. Bruck, P. Muellner, T. Schleder, R. Hainberger, M. Lammerhofer, *J. Biophotonics* 9 (2016) 218–223.
- [3] D. Gao, L. Wang, D. Lin, S.J. Yao, *Chromatogr. A.* 1294 (2013) 70–75.
- [4] Du, Q.; Lin, D.; Zhang, Q.; Yao, S. *J. Chromatogr. B.* 947–948 (2014) 201–207.
- [5] K.A. Kaleas, M. Tripodi, S. Revelli, V. Sharma, S.A.J. Pizarro, *Chromatogr. B.* 969 (2016) 256–263.
- [6] S.H.S. Mariam, C.W. Ooi, W.S. Tan, O.A. Janna, A. Arbakariya, B.T. They, *Separat. Purif. Technol.* 144 (2015) 133–138.
- [7] B. Akkaya, *Colloids Surf. B: Biointerfaces* 92 (2012) 151–155.
- [8] M. Haddad, C. Soukkarieh, H.E. Khalaf, A. Abbady, Q. De Gruyter, *Open* 11 (2016) 1–9.
- [9] Tong, H. F.; Lin, D. Q.; Chu, W. N.; ZHANG, Q. L.; Gao, D.; Wang, R. Z.; Yao, S. *J. J. Chromatogr. A.* 1429 (2016) 258–264.
- [10] A. Matschweiger, H. Engelmaier, G. Himmler, R.J. Hahn, *Chromatogr. B.* 1060 (2017) 53–62.
- [11] Luo, Y. D. Zhang, Q. L.; Yuan, X. M.; Shi, W.; Yao, S. J.; Lin, D. Q. *J. Chromatogr. B.* 1040 (2017) 105–111.
- [12] J.A. Anguizola, E.L. Pfaunmiller, M.L. Milanuk, D.S. Hage, *Methods.* 146 (2018) 39–45.
- [13] H.J. Heidebrecht, B. Kainz, R. Schopf, K. Godl, Z. Karcier, U. Kulozic, B.J. Förster, *Chromatogr. A.* 1562 (2018) 59–68.
- [14] X. Zou, Q. Zhang, H. Lu, D. Lin, S. Yao, *Chem. Eng. J.* 368 (2019) 678–686.



- [15] S. Bernardi, D. Gétaz, N. Forrer, M. Morbidelli, *J. Chromatogr. A* 1283 (2013) 46–52.
- [16] T. Besselink, A.E.M. Janssen, R.M. Boom, *Int. Dairy J.* 41 (2015) 32–37.
- [17] W.K. Chung, Y. Hou, M. Holstein, A. Freed, G.I. Makhatadze, S.M.J. Cramer, *Chromatogr. A* 1217 (2010) 191–198.
- [18] A. Hirano, T. Arakawa, T.J. Kameda, *Chromatogr. A* 1338 (2014) 58–66.
- [19] A. Nascimento, I.F. Pinto, V. Chu, M.R. Aires-Barros, J.P. Conde, *Separat. Purif. Technol.* 195 (2018) 388–397.
- [20] Y. Yang, X.J. Geng, *Chromatogr. A* 1218 (2011) 8813–8825.
- [21] J. Yan, Q.L. Zhang, D.Q. Lin, S.J.J. Yao, *Chem. Eng.* 61 (2016) 151–159.
- [22] A.K. Dutta, D. Fedorenko, J. Tan, J.A. Costanzo, D.S. Kahn, A.L. Zydney, O.J. Shinkazh, *Chromatogr. A* 1511 (2017) 37–44.
- [23] S. Maria, G. Joucla, B. Garbay, W. Dieryck, A. Lomenech, X. Santarelli, C.J. Cabanne, *Chromatogr. A* 1393 (2015) 57–64.
- [24] E. O'connor, M. Aspelund, F. Bartnik, M. Berge, K. Coughlin, M. Kambarami, D. Spencer, H. Yan, W.J. Wang, *Chromatogr. A* 1499 (2017) 65–77.
- [25] Lima, M. A.; Freitas, M. F. M.; Gonçalves, L. R. B.; Silva Jr., I. J. *Chromatogr. B* 1015–1016 (2016) 181–191.
- [26] Y.D. Luo, Q.L. Zhang, X.M. Yuan, W. Shi, S.J. Yao, D.Q.J. Lin, *Chromatogr. B* 1040 (2017) 105–111.
- [27] I.T.L. Bresolin, M.C.M. Souza, S.M.A.J. Bueno, *Chromatogr. B* 878 (2010) 2087–2093.
- [28] C.J. Geankoplis, *Transport Processes and Separation Process Principles (Includes Unit Operations)*, 4. ed., Prentice Hall Press, New Jersey, 2003.
- [29] gPROMS, Version 3.2.0, User Guide, (2009).
- [30] M.M. Bradford, A rapid and sensitive method for the quantitation of microgram quantities of protein utilizing the principle of protein-dye binding, *Anal. Biochem.* 72 (1976) 248–254.
- [31] U.K. Laemmli, Cleavage of structural proteins during assembly of head of bacteriophage-T4, *Nature* 227 (1970) 680–685.
- [32] Joucla, G.; Sénéchal, C. L.; Bégorre, M.; Garbay, B.; Santarelli, X.; Cabanne, C. J. *Chromatogr. B* 942–943 (2013) 126–133.
- [33] A.M. Gospodarek, D.E. Hiser, J.P. O'connell, E.J.J. Fernandez, *Chromatogr. A* 1355 (2014) 238–252.
- [34] M.A. Lima, *Recovery and Purification of  $\beta$ -Galactosidase From *Kluyveromyces lactis* Using Mixed Mode Chromatography (MSc Dissertation)*, Federal University of Ceará, 2014.
- [35] M. Zhu, G. Carta, *Adsorpt.* 22 (2016) 165–179.
- [36] F. Bazzaz, E. Binaeian, A. Heydarinasab, A. Ghadi, *Adv. Powder Technol.* 29 (2018) 1664–1675.
- [37] Ö. Acet, B. Önal, R. Sanz, E.S.S. Pérez, D. Erdönmez, M. Odabaşı, *J. of Molec. Liq.* 276 (2019) 480–487.
- [38] Y. Li, Y.J. Sun, *Chromatogr. A* 1373 (2014) 97–105.
- [39] J. Yan, Q.L. Zhang, D.Q. Lin, S.J.J. Yao, *Sep. Sci.* 37 (2014) 2474–2480.
- [40] H.F. Tong, D.Q. Lin, X.M. Yuan, S.J.J. Yao, *Chromatogr. A* 1244 (2012) 116–122.
- [41] R.Z. Wang, D.Q. Lin, H.F. Tong, X.M. Yuan, H.L. Lu, S.J.J. Yao, *Chromatogr. B* 936 (2013) 33–41.
- [42] T. Barroso, M. Temtem, A. Hussain, A. Aguiar-Ricardo, A.C.A.J. Roque, *Membr Sci* 348 (2010) 224–230.